Electronic supplementary materials

Highly selective sensing of Fe^{3+}/Hg^{2+} and proton conduction using two fluorescent Zn(II) coordination polymers

Tian-Yang Xu[a,b], Hong-Jiao Nie[c*], Jia-Ming Li[a*], Zhong-Feng Shi[a,b*]

[a] Guangxi Colleges and Universities Key Laboratory of Beibu Gulf Oil and Natural Gas Resource Effective Utilization, College of Petroleum and Chemical Engineering, Beibu Gulf University, Qinzhou 535011 People's Republic of China

[b] School of Chemistry and Pharmacy, Guangxi Normal University, Key Laboratory for the Chemistry and Molecular Engineering of Medicinal Resources (Ministry of Education), Guilin 541004 People's Republic of China

[c] Key Laboratory of Functional Nanomaterials and Technology in Universities of Shandong, School of Chemistry and Chemical Engineering, Linyi University, Linyi 276000 People's Republic of China

[*]Corresponding authors: Jia-Ming Li, e-mail: jmli@bbgu.edu.cn; Hong-Jiao Nie, e-mail: niehongjiao@lyu.edu.cn; Zhong-Feng Shi, e-mail: shizhongfeng01@163.com

Table S1. Selected Bond lengths [Å] and angles [°] for polymer **1** and **2**.

Polymer **1**			
Zn1—O1	1.9635 (18)	Zn1—N1	2.007 (2)
Zn1—O4^{i}	1.9852 (19)	Zn1—N4^{ii}	1.998 (2)
O1—Zn1—O4^{i}	108.43 (8)	O4^{i}—Zn1—N4^{ii}	103.37 (8)
O1—Zn1—N4^{ii}	122.61 (8)	O4^{i}—Zn1—N1	112.60 (8)
O1—Zn1—N1	100.80 (8)	N4^{ii}—Zn1—N1	109.29 (9)
Polymer **2**			
Zn1—O9	1.969 (2)	Zn3—N1	1.988 (3)
Zn1—O	2.079 (2)	Zn3—N12^{ii}	2.025 (3)
Zn1—O1	2.075 (2)	Zn3—N4^{iii}	1.995 (3)
Zn1—O3	1.966 (2)	Zn2—O10	1.966 (3)
Zn1—N8^{i}	2.048 (3)	Zn2—O8^{iv}	1.963 (2)
Zn3—O2	1.992 (3)	Zn2—N9	1.998 (3)
Zn3—N5	1.996 (3)		
O9—Zn1—O7	87.30 (9)	O2—Zn3—N12^{ii}	105.71 (11)
O9—Zn1—O1	88.38(10)	O2—Zn3—N4^{iii}	104.59 (13)
O9—Zn1—N8^{i}	116.90 (12)	N1—Zn3—O2	111.14 (12)
O1—Zn1—O7	168.39 (10)	N1—Zn3—N12^{ii}	106.35 (12)
O3—Zn1—O9	136.69 (11)	N1—Zn3—N4^{iii}	121.07 (12)
O3—Zn1—O7	88.35 (10)	N4^{iii}—Zn3—N12^{ii}	106.99 (12)
O3—Zn1—O1	87.42 (10)	O10—Zn2—N9	113.12 (12)
O3—Zn1—N8^{i}	106.39 (12)	O10—Zn2—N5	104.43 (13)
N8^{i}—Zn1—O7	94.52 (11)	O8^{iv}—Zn2—O10	95.61 (11)
N8^{i}—Zn1—O1	97.04 (11)	O8^{iv}—Zn2—N9	119.77 (12)
O8^{iv}—Zn2—N5	110.91 (13)	N5—Zn2—N9	111.09 (13)

Symmetry codes **1**: (i) x-1, y, z; (ii) x-1, y, z-1; (iii) x+1, y, z; (iv) x+1, y, z+1.

Symmetry codes **2**: (i) x+1, 1/2-y, z+1/2; (ii) x+1, y, 1+z; (iii) 1-x, 1/2+y, 3/2-z; (iv) 1-x, 1-y, 1-z; (v) x-1, y, z-1; (vi) 1-x, y-1/2, 3/2-z; (vii) x-1, 1/2-y, z-1/2.

Table S2. Hydrogen bonding parameters of **1**.

D—H···*A*	*D*—H	H···*A*	*D*···*A*	*D*—H···*A*
O3—H3···O2	0.82	1.85	2.574 (3)	146
O7—H7A···O4	0.85	2.18	3.026 (3)	176
O7—H7B···O6^{i}	0.85	2.41	3.168 (4)	150

Table S3. Hydrogen bonding parameters of **2**.

D—H···*A*	*D*—H	H···*A*	*D*···*A*	*D*—H···*A*
O13—H13A···O6	0.85	1.97	2.807 (6)	167.3
O13—H13B···O14	0.85	1.97	2.816 (10)	170.3
O16—H16B···O2	0.85	2.16	2.999(6)	166.9
O14—H14A···O15	0.85	1.81	2.62(2)	158.5
O17—H17A···O5	0.85	2.08	2.923 (11)	173.5

Table S4. The CIE coordinates of the **1** and **1** ***@*** M^{n+} in maximum emissions of **1** ((λ_{ex} =323nm). The CIE coordinates of the **2** and **2** ***@*** M^{n+} in maximum emissions of **2** ((λ_{ex} =311nm).

Compound **1**	CIE coordinates	Compound **2**	CIE coordinates
1 @ Ag^{+}	(0.15, 0.06)	**2** @ Ag^{+}	(0.16, 0.04)
1 @ Al^{3+}	(0.15, 0.05)	**2** @ Al^{3+}	(0.15, 0.02)
1 @ Ca^{2+}	(0.15, 0.06)	**2** @ Ca^{2+}	(0.16, 0.04)
1 @ Cd^{2+}	(0.15, 0.06)	**2** @ Cd^{2+}	(0.16, 0.04)
1 @ Co^{2+}	(0.15, 0.06)	**2** @ Co^{2+}	(0.16, 0.04)
1 @ Cr^{3+}	(0.15, 0.06)	**2** @ Cr^{3+}	(0.16, 0.04)
1 @ Cu^{2+}	(0.15, 0.06)	**2** @ Cu^{2+}	(0.16, 0.03)
1 @ Fe^{3+}	(0.15, 0.04)	**2** @ Fe^{3+}	(0.16, 0.01)
1 @ Hg^{2+}	(0.15, 0.05)	**2** @ Hg^{2+}	(0.13, 0.03)
1 @ K^{+}	(0.15, 0.06)	**2** @ K^{+}	(0.16, 0.04)
1 @ Li^{+}	(0.15, 0.06)	**2** @ Li^{+}	(0.16, 0.04)
1 @ Mg^{2+}	(0.15, 0.06)	**2** @ Mg^{2+}	(0.16, 0.04)
1 @ Mn^{2+}	(0.15, 0.06)	**2** @ Mn^{2+}	(0.16, 0.04)
1 @ Ni^{2+}	(0.15, 0.06)	**2** @ Ni^{2+}	(0.16, 0.04)
1 @ Pb^{2+}	(0.15, 0.06)	**2** @ Pb^{2+}	(0.16, 0.04)
1 @ Zn^{2+}	(0.15, 0.05)	**2** @ Zn^{2+}	(0.16, 0.04)
blank	(0.15, 0.06)	blank	(0.16, 0.04)

Table S5. Comparison of detection capacities of **1** towards Fe^{3+} ion with other materials.

Materials	$K_{sv}(M^{-1})$	Detection limit	Ref.
$\{[Zn_2(\mu_4\text{-}L)(\mu_3\text{-}bta(3H_2O)]\cdot H_2O\}_n$	1.06×10^4	1.1 mM	1
$\{[Zn(L)_{0.5}(bimb)]\cdot 2H_2O\cdot 0.5(CH_3)_2NH\}_n$	6.28×10^4	0.48 μM	2
$\{[Zn(L)_{0.5}(btdpe)]\cdot H_2O\}_n$	4.07×10^4	0.74 μM	2
$[Zn_3(DDB)(DPE)]\cdot H_2O$	5.0×10^4	1.8×10^{-7} M	3
$Tb(HL)(H_2O)_2$	1.37×10^4	7.74×10^{-4} mM	4
$[Zn(modbc)_2]_n$(Zn-CP)	7.20×10^3	0.57 mM	5
534-MOF-Tb	5.51×10^3	0.13 mM	6
$[Zn(L)_2]_n$	1.34×10^4	2.24 μM	7
Eu^{3+}@MIL-53-COOH (Al)	5.12×10^3	0.5 μM	8
Benzimidazole-based sensor	8.51×10^4	2 μM	9
BUT-14	2.17×10^3	3.8 μM	10
BUT-15	1.66×10^4	0.8μM	10
$Eu_2(MFDA)_2(HCOO)_2(H_2O)_6$	1.58×10^3	0.3 μM	11
1	4.16×10^4	1.66 μM	This work

Table S6. Comparison of detection capacities of **2** towards Hg^{2+} ion with other materials.

Materials	$K_{sv}(M^{-1})$	Detection limit	Ref.
$[Cd(L)(NTA)]_n$	3.57×10^3	3.05 μM	12
$[Ni(L)(NPTA)\cdot H_2O]_n$	7.43×10^3	2.29 μM	12
$[Cd(2\text{-}NH_2bdc)(tib)\cdot 4H_2O\cdot 0.5DMA]_n$	-	4.2×10^{-8} M	13
$\{[Cd(BIPA)(tfbdc)(H_2O)]\cdot DMF\}_n$	1.27×10^4	1.2×10^{-7} M	14
RuUiO-67	-	0.5 μM	15
$[Zn_2(bbmb)_2(tdc)_2]\cdot 2H_2O$	4.81×10^5	0.19 μM	16
TbTATAB	-	4.4 nM	17
2	1.98×10^5	0.23 μM	This work

Table S7. The ICP result of polymer **2** with Hg^{2+} for 6 hours.

Polymer **2**	Concentration /μM
Initial value / Hg^{2+}	0.82
Immersion of Hg^{2+} ions for 6 hours	0.46

Table S8. The proton conductivity of polymer **1** and **2** at 10 °C with different humidities.

Relative humidity (% RH)	Polymer **1** ($S \cdot cm^{-1}$)	Polymer **2** ($S \cdot cm^{-1}$)
45% RH	4.40×10^{-7}	4.68×10^{-7}
53% RH	5.51×10^{-7}	5.92×10^{-7}
62% RH	5.84×10^{-7}	6.67×10^{-7}
71% RH	9.51×10^{-7}	7.51×10^{-7}
83% RH	1.68×10^{-6}	8.01×10^{-7}
95% RH	7.87×10^{-6}	8.81×10^{-7}

Table S9. The proton conductivity of polymer **1** and **2** at 95% RH with different temperature.

Temperature	Polymer **1** ($S \cdot cm^{-1}$)	Polymer **2** ($S \cdot cm^{-1}$)
10℃	7.87×10^{-6}	8.81×10^{-7}
20℃	9.76×10^{-6}	1.49×10^{-6}
30℃	1.43×10^{-5}	2.21×10^{-6}
40℃	2.03×10^{-5}	3.69×10^{-6}
50℃	2.91×10^{-5}	4.79×10^{-6}
60℃	3.45×10^{-5}	6.26×10^{-6}

Table S10. Summarized proton conductivities of some MOFs at high humidity (>80% RH)

Materials	Proton conductivity ($S \cdot cm^{-1}$)	RH and Temperature (°C)	Ref.
MIL-53(Fe)$(COOH)_2$	1.5×10^{-3}	95% and 80	18
$[Cd(L\text{-tart})\text{-}(bpy)(H_2O)]_n \cdot 9n(H_2O)$	1.3×10^{-6}	95% and 85	19
$[Cd(D\text{-tart})\text{-}(bpy)(H_2O)]_n \cdot 9n(H_2O)$	1.3×10^{-6}	95% and 85	19
$[Cd(DL\text{-tart})\text{-}(bpy)(H_2O)]_n \cdot 6n(H_2O)$	4.5×10^{-7}	95% and 85	19
$\{[Gd(L)(Ox)(H_2O)]_n \cdot 3H_2O\}$	4.7×10^{-4}	95% and 80	20
Tb-DSOA	4.0×10^{-4}	98% and 53	21
β-PCMOF2	1.8×10^{-6}	85% and 50	22
PCMOF2	2.4×10^{-5}	85% and 50	22
PCMOF-3	3.5×10^{-5}	98% and 25	23
Sr-SBBA	4.4×10^{-5}	98% and 25	24
$[La_2(ox)_3(H_2O)_6]\ 4H_2O$	3.35×10^{-7}	100% and 95	25
$[Zn_2(HCOO)(trz)_3]_n$	7.95×10^{-7}	98% and 50	26
1	3.45×10^{-5}	95% and 60	This work
2	6.26×10^{-6}	95% and 60	This work

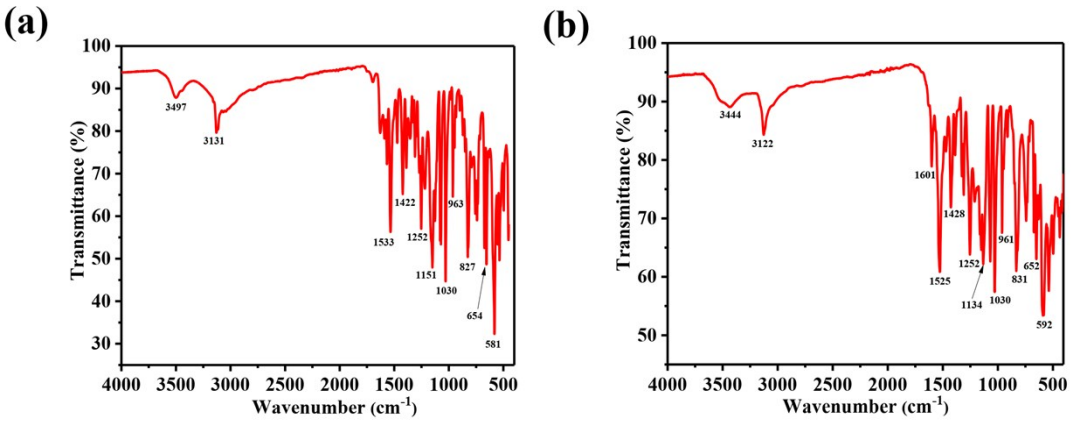

Fig. S1 (a) The IR spectra of **1**. (b) The IR spectra of **2**.

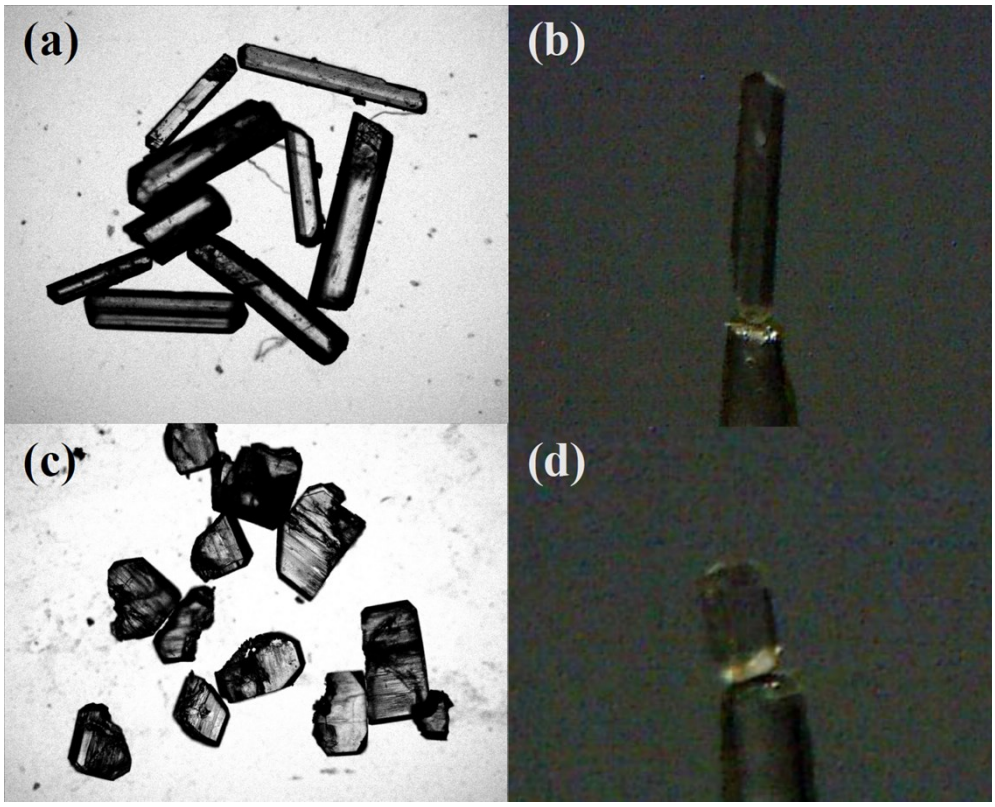

Fig. S2 Sample crystal photographs of polymer **1** (a) and polymer **2** (c). Single-crystal photographs of polymer **1** (b) and polymer **2** (d).

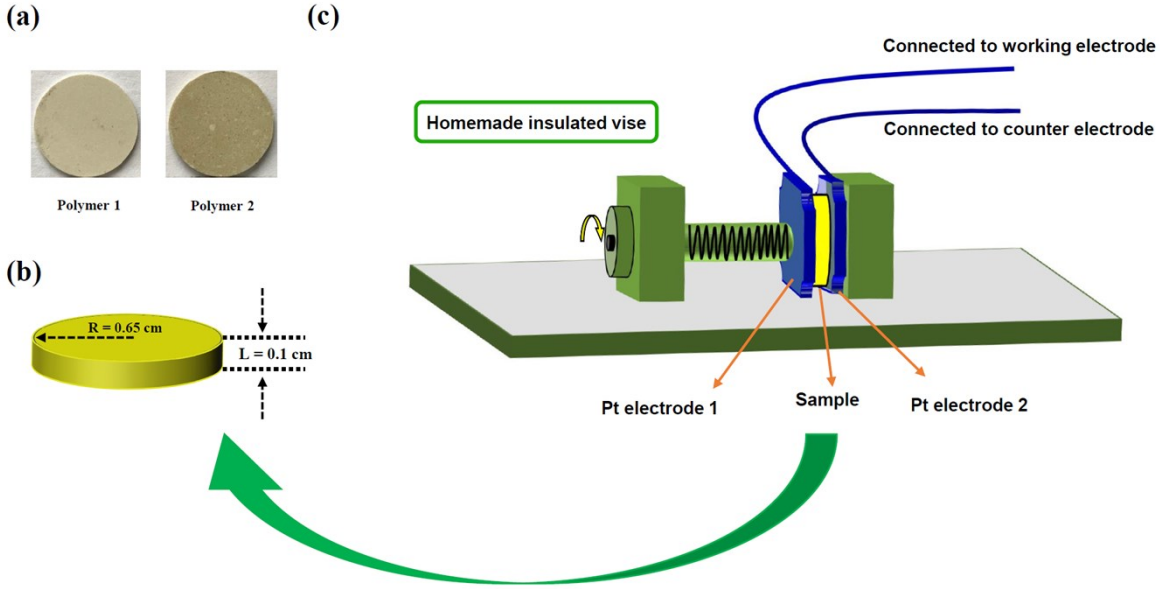

Fig. S3 (a) Photographs of wafer press plates for polymers **1** and **2**; (b) schematic diagram of wafer samples used for proton conductivity; (c) the home-made device for a proton conductivity test.

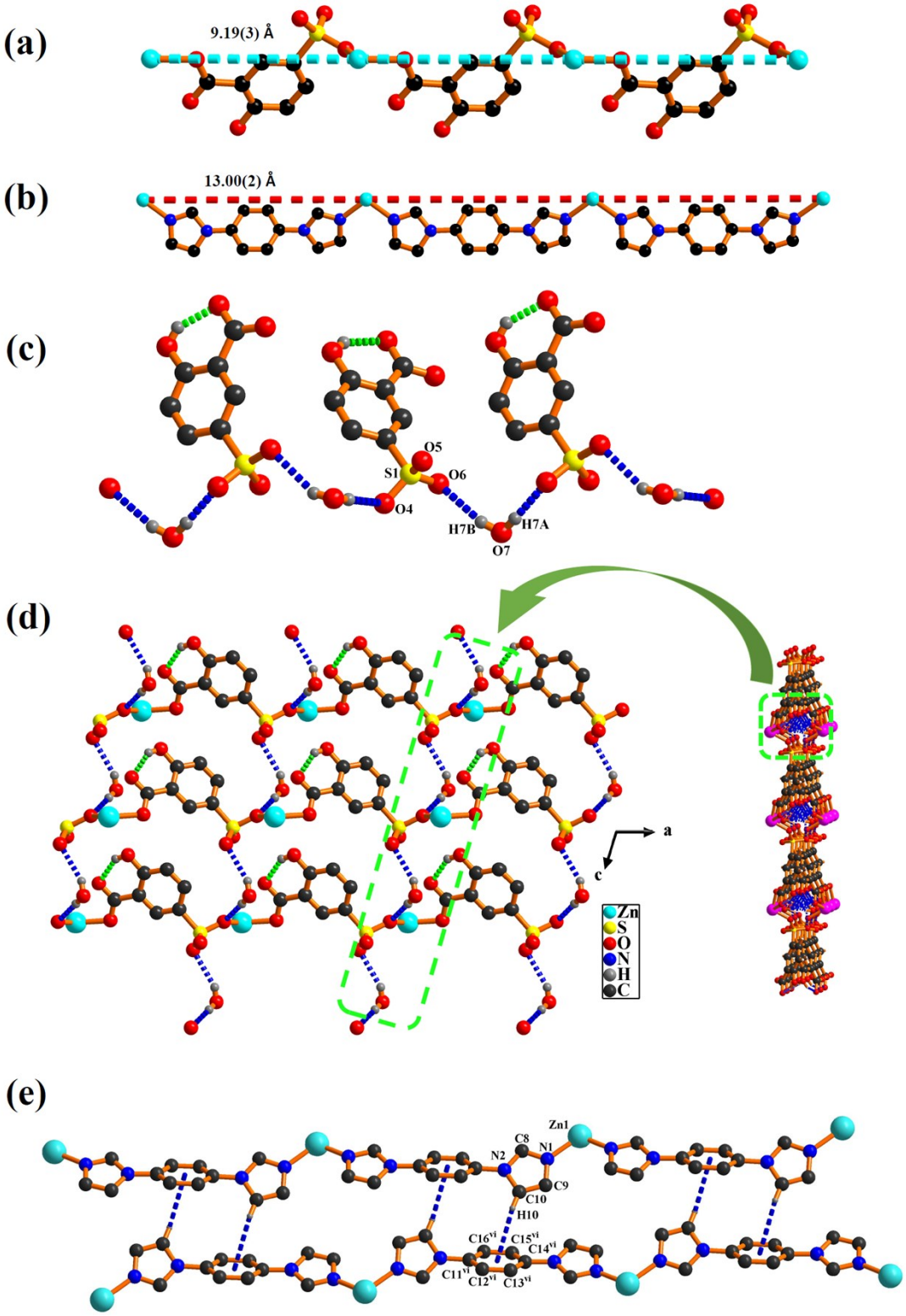
(a)
9.19(3) Å
(b)
13.00(2) Å
(c)
O5
S1
O6
O4
H7B
H7A
O7
(d)
a
c
Zn
S
O
N
H
C
(e)
Zn1
C8
N1
N2
C9
C10
H10
C16vi
C15vi
C14vi
C11vi
C12vi
C13vi

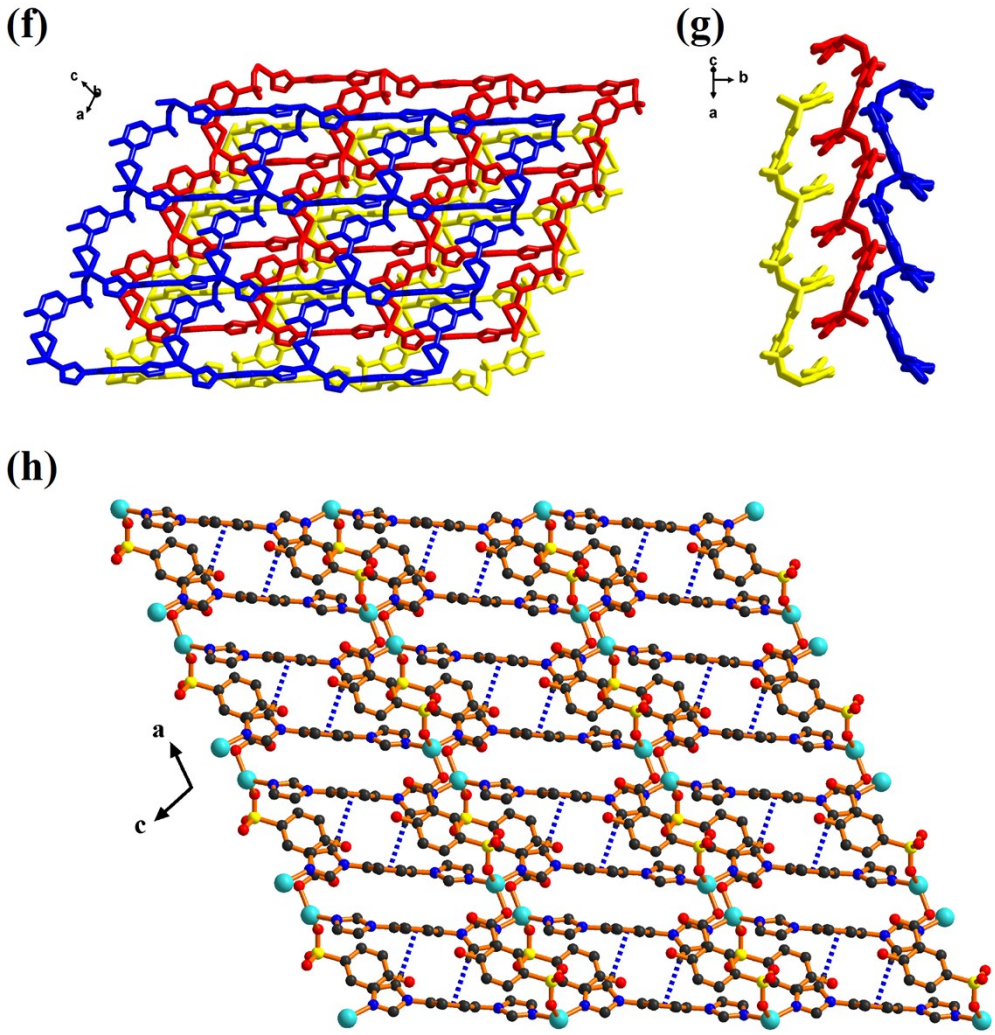

Fig. S4 (a) The 1D $[Zn(H_3ssa)_n]$ chain in polymer **1**; (b) the 1D $[Zn(1,4\text{-bib})_n]$ chain in polymer **1**; (c) the hydrogen-bonded passageway of polymer **1**; (d) the 2D H-bonged framework; (e) the C-H···π interactions of polymer **1**; (f) the 3D structure framework of polymer **1** viewed in the direction *b*; (g) the 3D structure framework of polymer **1** viewed in the vertical *b* direction; (h) the 2D C-H···π interactions of polymer **1**.

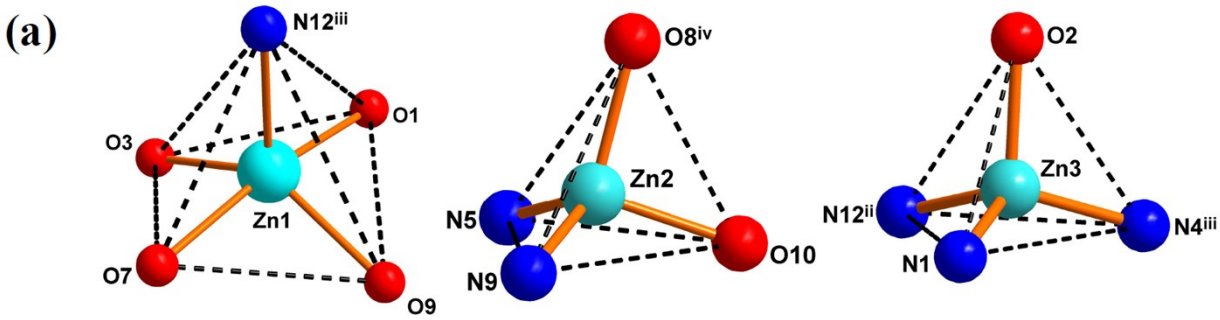

(b)

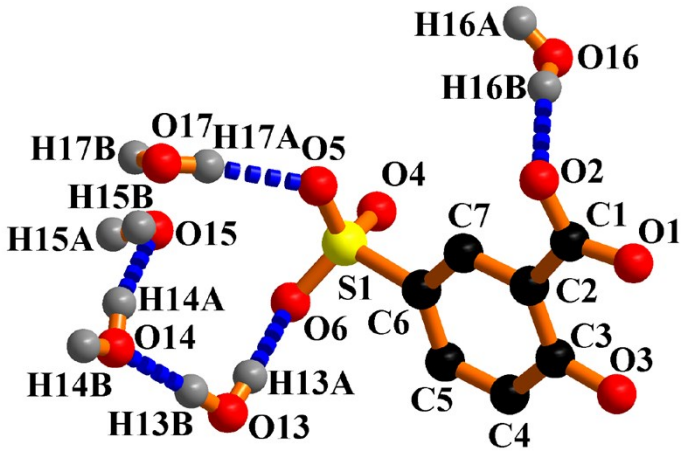
H16A
O16
H16B
O2
C1
O1
C7
C2
C3
O3
C4
C5
C6
S1
O4
O5
O6
H17B
O17
H17A
H15B
H15A
O15
H14A
O14
H14B
H13A
H13B
O13

(c)

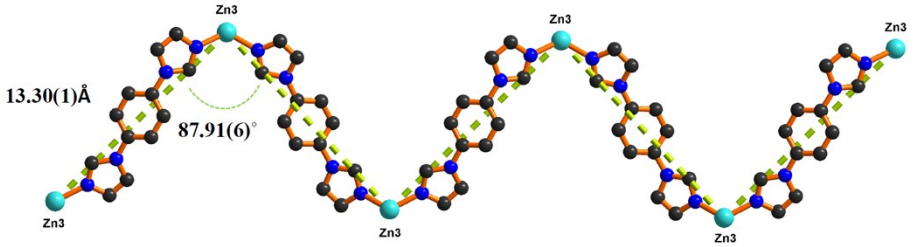
Zn3
Zn3
Zn3
Zn3
Zn3
Zn3
13.30(1)Å
87.91(6)°

(d)

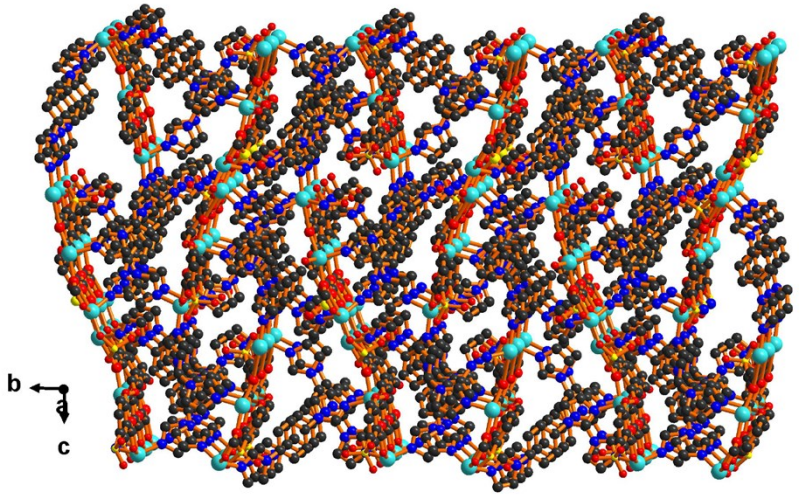
b
a
c

(e)

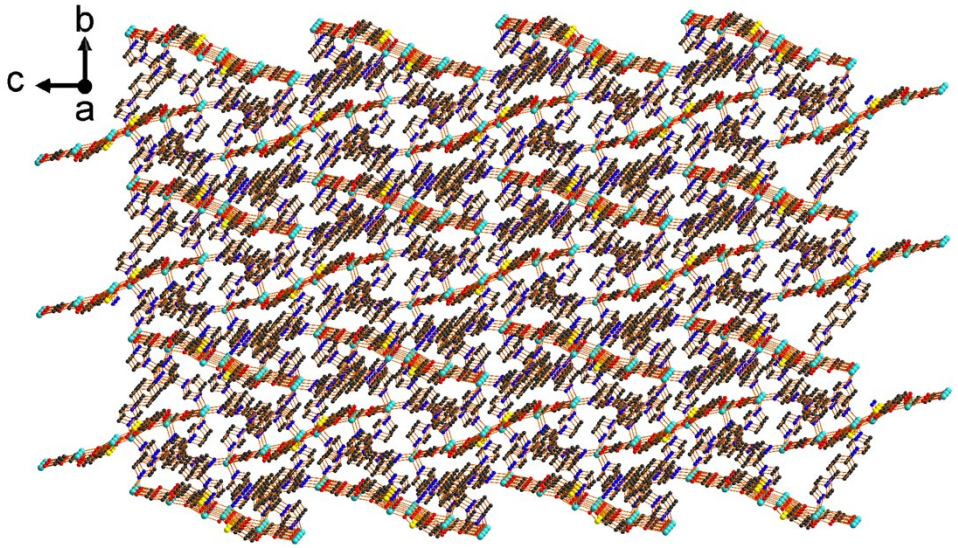
b
c
a

Fig. S5 (a) Polyhedral view of polymer **2**; (b) The intermolecular O–H···O hydrogen bonds in polymer **2**. (c) the 1D [Zn(1,4-bib)$_n$] chain in polymer **2**; (d) the first simplified method of polymer **2**, and the 3D structural framework corresponding to the topology; (e) the second simplified method of polymer **2**, and the 3D structural framework corresponding to the topology.

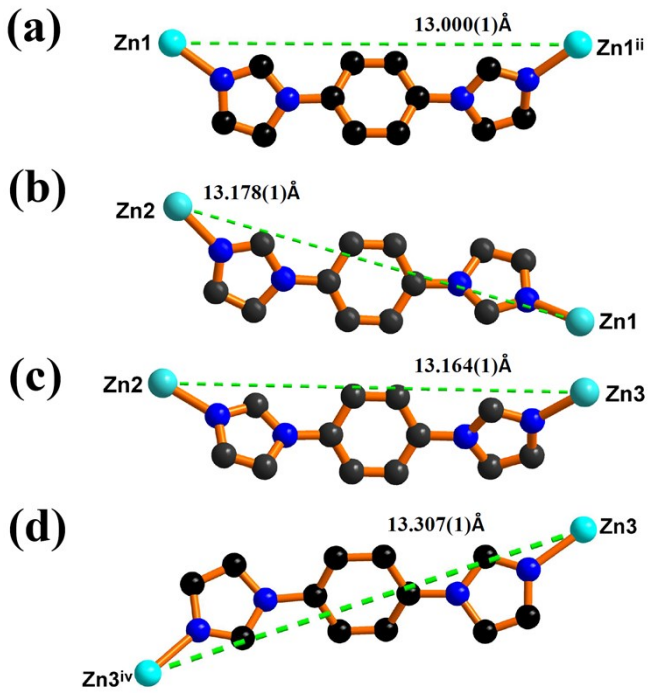

Fig. S6 (a) The 1,4-bib ligand connector of the polymer **1**; (b-d) the 1,4-bib ligand connector of the polymer **2**.

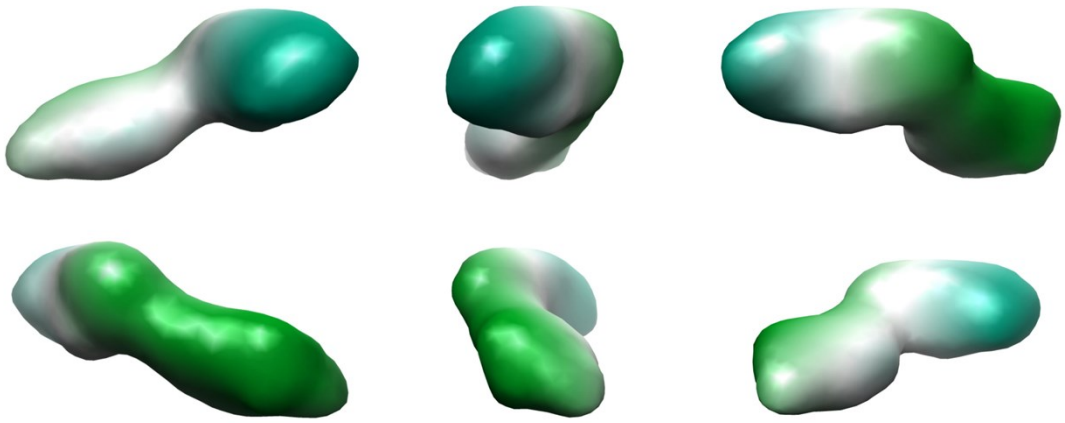

(a)

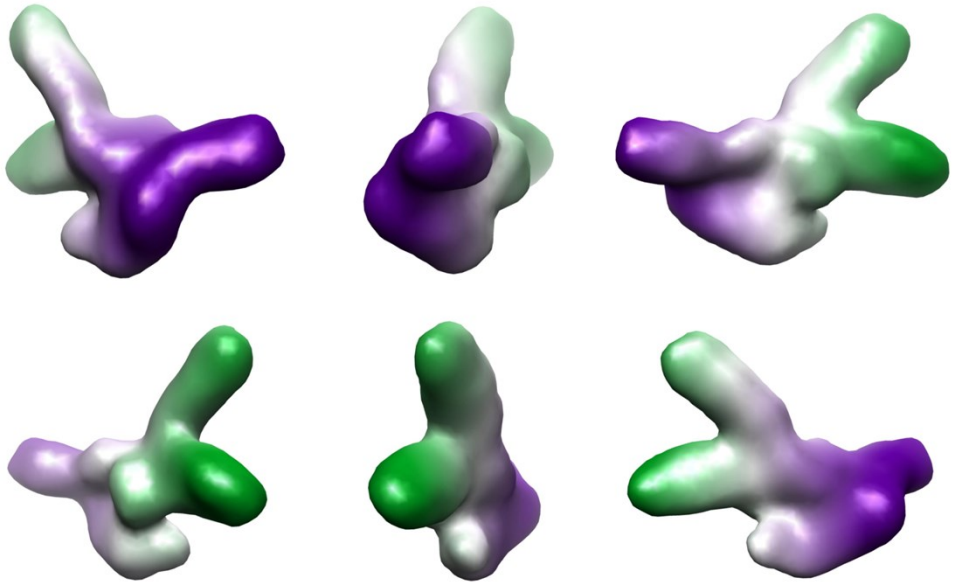

(b)

Fig. S7 The surface of **1** (a) and **2** (b) calculated via 3V Volume Assessor program by rolling a virtual probe (0.8 Å) on the surface viewed along six different orientations.

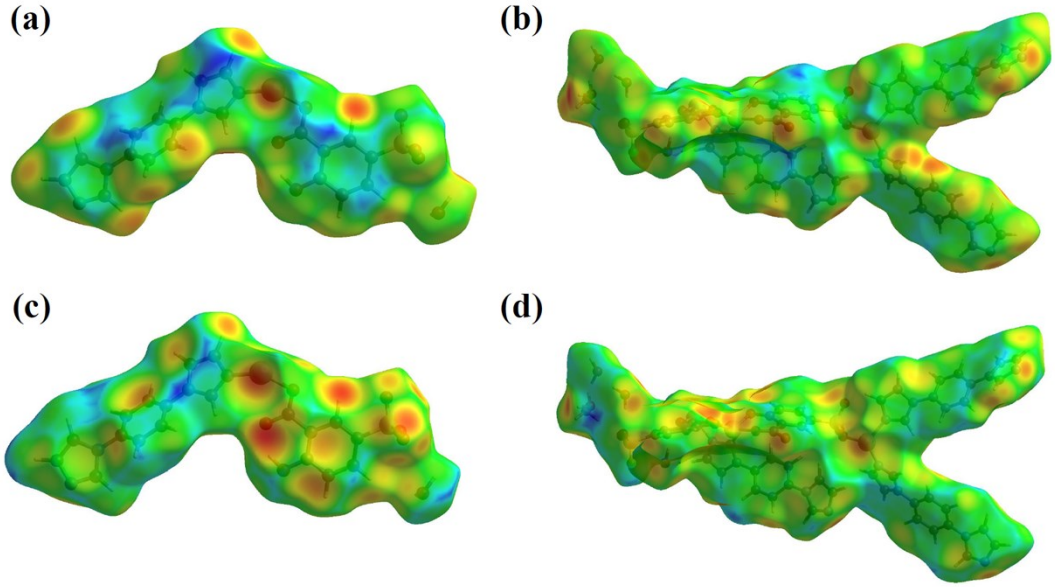

Fig. S8 Hirshfeld surface of polymer **1** with d_i (a), d_e (c) mapped in colour; the Hirshfeld surface of polymer **2** with d_i (b), d_e (d) mapped in colour; in all cases, red represents the closest contacts, and blue the most distant contacts.

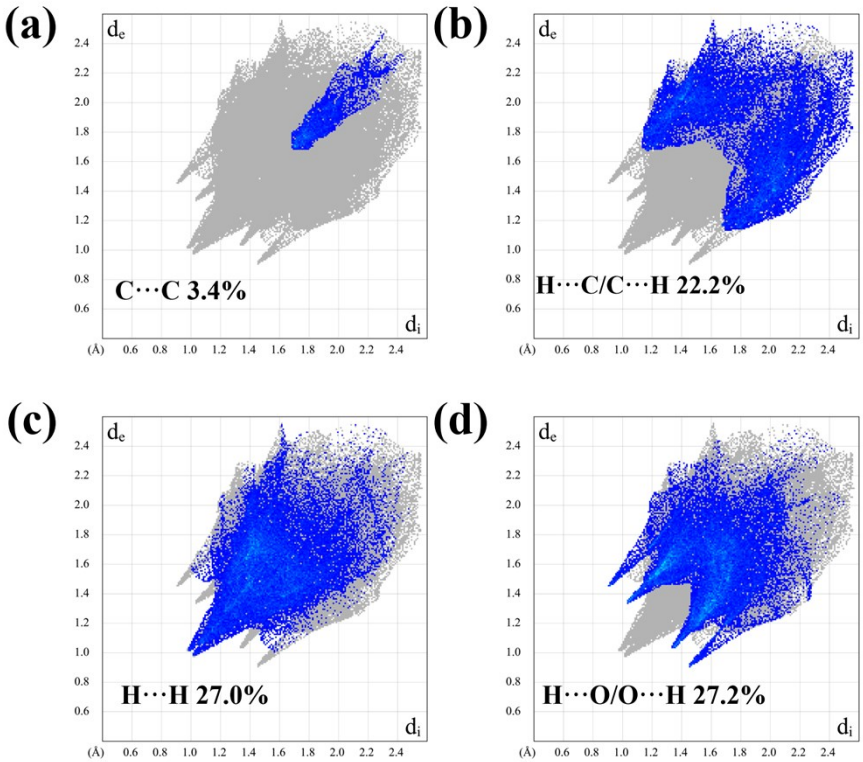

Fig. S9 Fingerprint plot of polymer **1**: resolved into C···C (a), H···C/C···H (b), H···H (c), and H···O/O···H (d) contacts showing the percentages of contacts contributed to the total Hirshfeld surface area of the molecule.

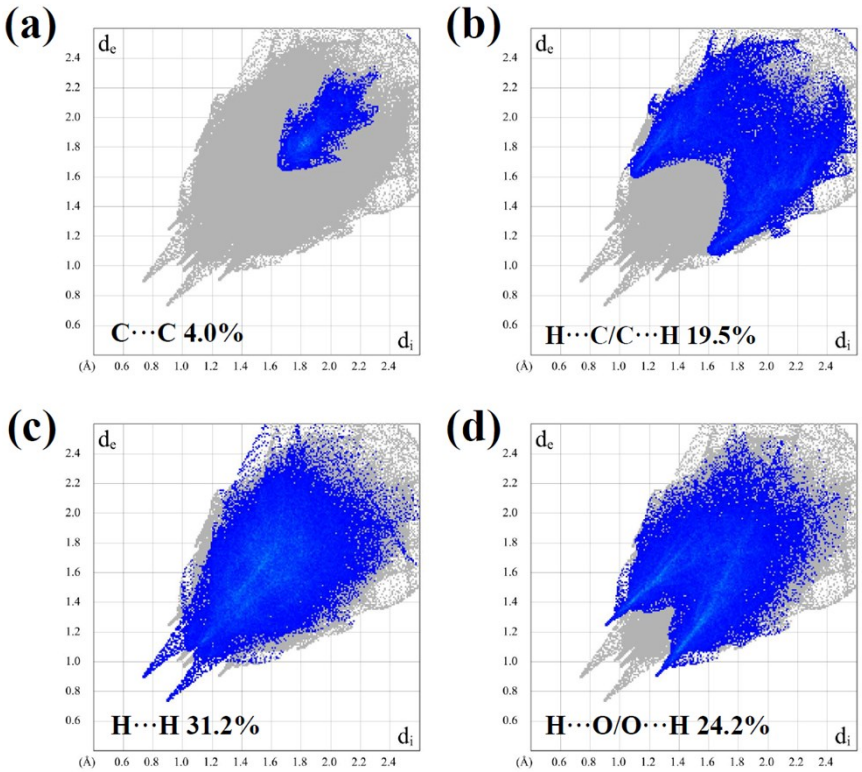

Fig. S10 Fingerprint plot of polymer **2**: resolved into C···C (a), H···C/C···H (b), H···H (c), and H···O/O···H (d) contacts showing the percentages of contacts contributed to the total Hirshfeld surface area of the molecule.

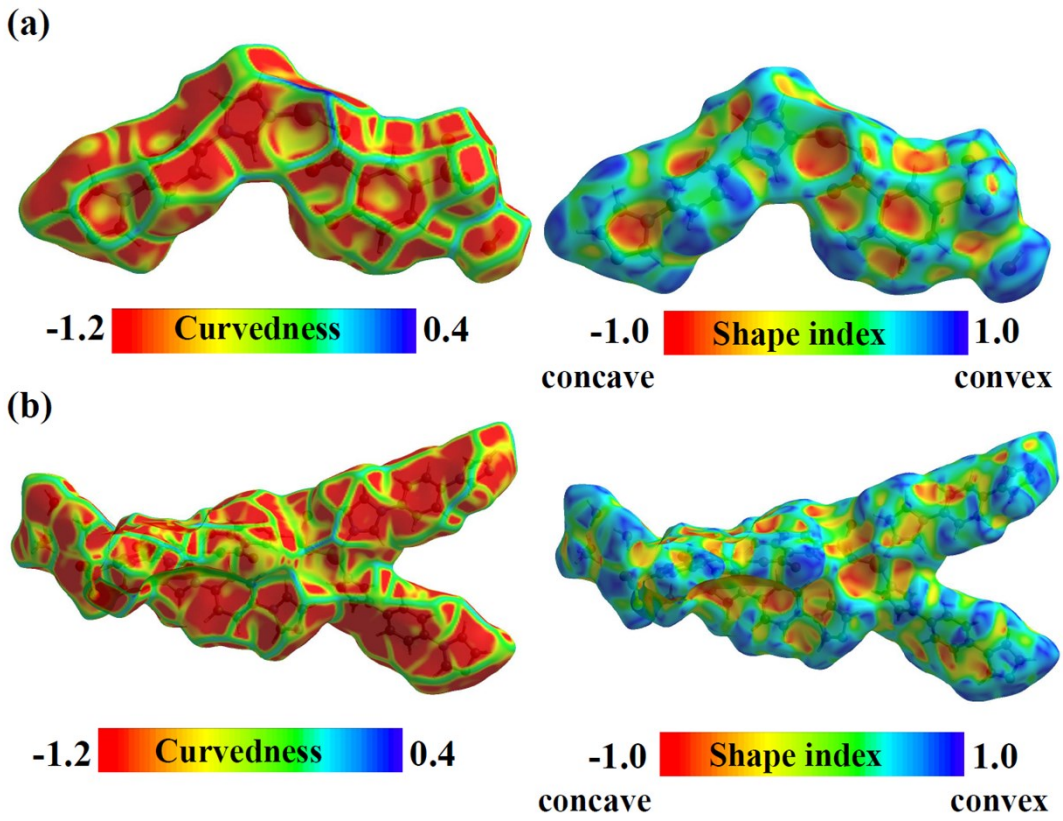

Fig. S11 (a) Hirshfeld surface of polymer **1** with curvedness and shape index mapping; (b) the Hirshfeld surface of polymer **2** with curvedness and shape index mapping.

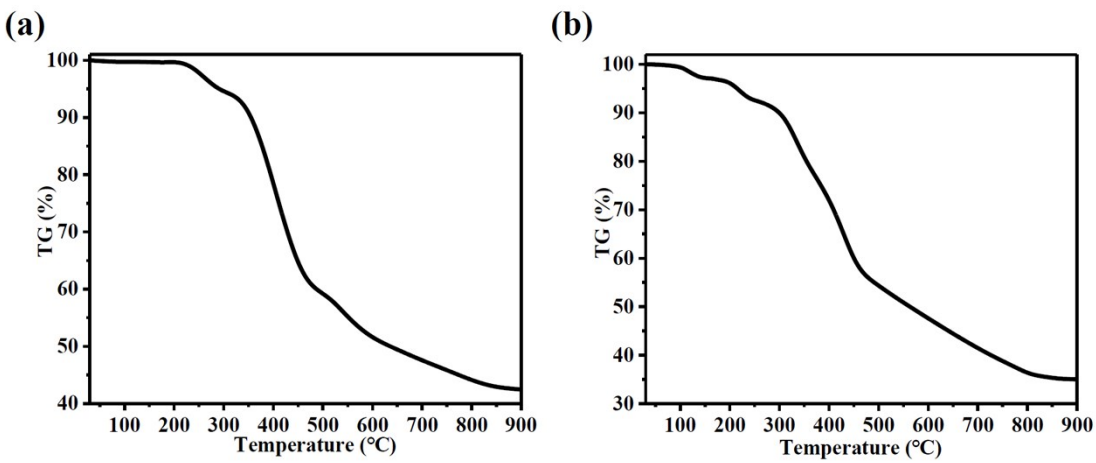

Fig. S12 The TG curves for **1** (a) and **2** (b).

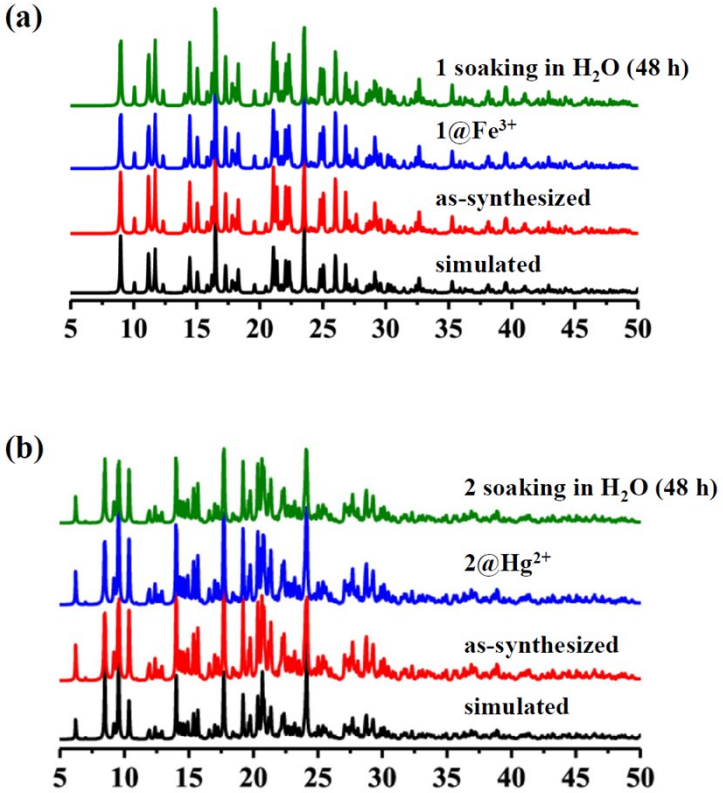

Fig. S13 The PXRD patterns of polymers **1** and **2**.

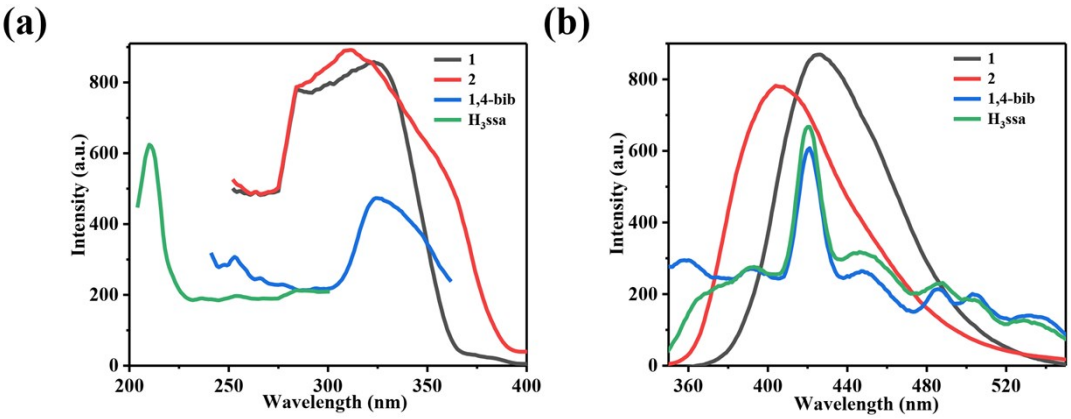

Fig. S14 (a) The solid-state excitation spectra of H_3ssa (λ_{ex} = 210 nm), 1,4-bib (λ_{ex} = 324 nm), **1** (λ_{ex} = 323 nm), and **2** (λ_{ex} = 311 nm) at room temperature, (b) the solid-state emission spectra of H_3ssa (λ_{em} = 420 nm), 1,4-bib (λ_{em} = 420 nm), **1** (λ_{em} = 425 nm), and **2** (λ_{em} = 405 nm) at room temperature.

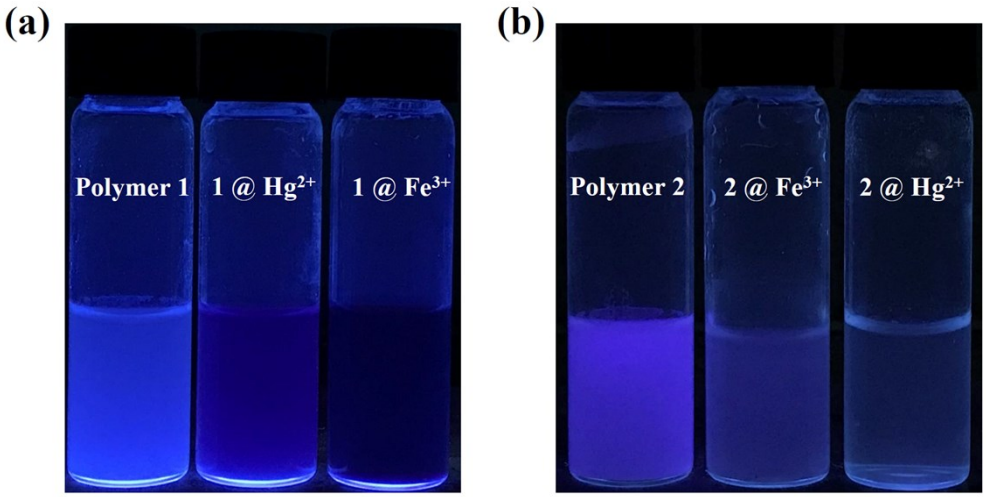

Fig. S15 (a) The photograph of polymer **1**, **1**@Hg^{2+}, and **1**@Fe^{3+} samples in water under UV light of 300 nm; (b) the photograph of polymer **2, 2**@Fe^{3+}, and **2**@Hg^{2+} samples in water under UV light of 365 nm.

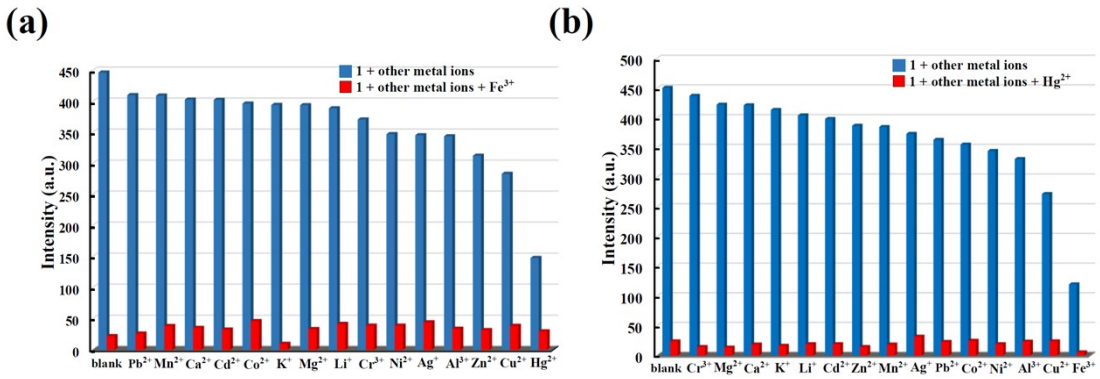

Fig. S16 (a) The relative emission intensity of polymer **1** before and after addition Fe^{3+} (1.5ml, 10^{-3} M) and other metal ions (1.5ml,10^{-3} M); (b) the relative emission intensity of polymer **2** before and after addition Hg^{2+} (1.5ml, 10^{-3} M) and other metal ions (1.5ml,10^{-3} M).

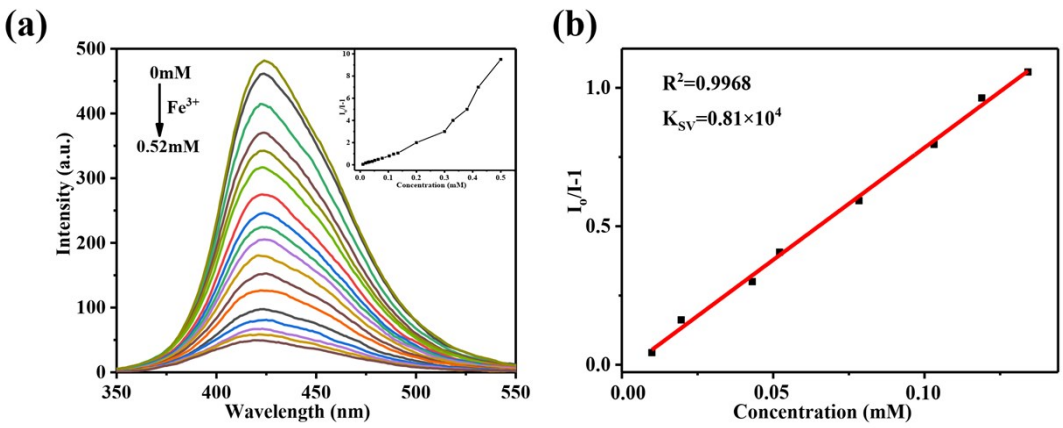

Fig. S17 (a) Fluorescent spectra of polymer **1** in simulated biological systems in the presence of different concentrations of Fe^{3+} at 37℃; (b) emission quenching linearity relationship at low concentrations of Fe^{3+} ion for polymer **1** in simulated biological systems.

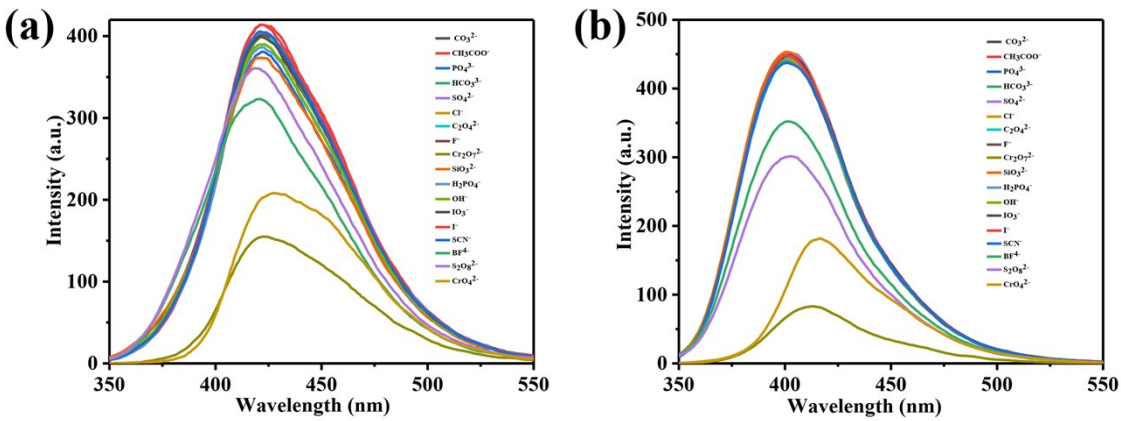

Fig. S18 The photoluminescence spectra for polymer **1** (a) and **2** (b) in aqueous solution with various anions.

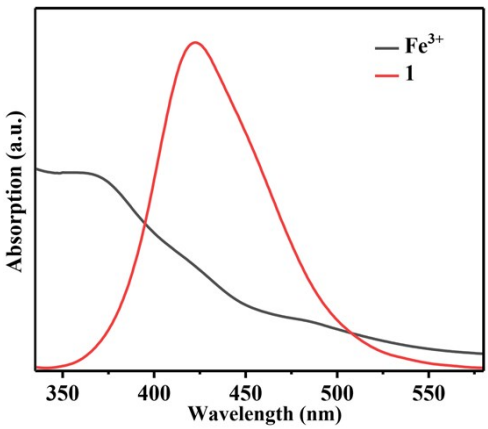

Fig. S19 UV-Vis absorption spectra of Fe^{3+} in aqueous solution.

the emission spectrum of polymer **1** dispersed in water upon excitation of 323 nm.

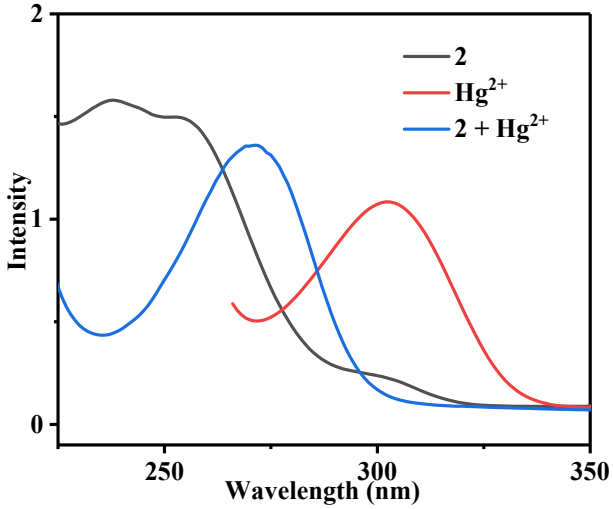

Fig. S20 UV-vis spectra of polymer **2** before and after addition of Hg^{2+} ion.

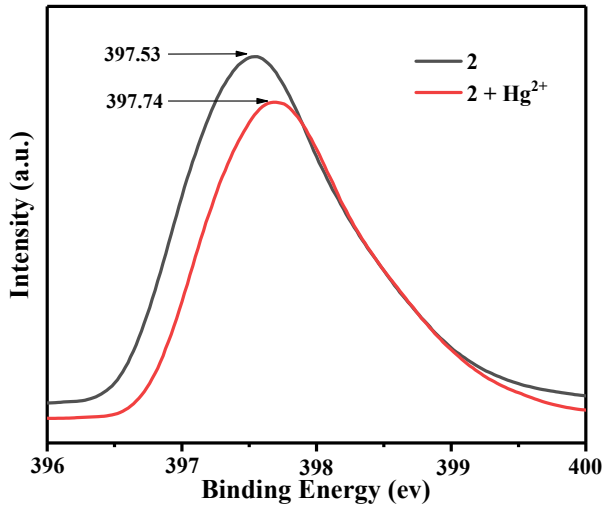

Fig. S21 N 1s XPS spectra of polymer **2** before and after immersed in Hg^{2+} ion.

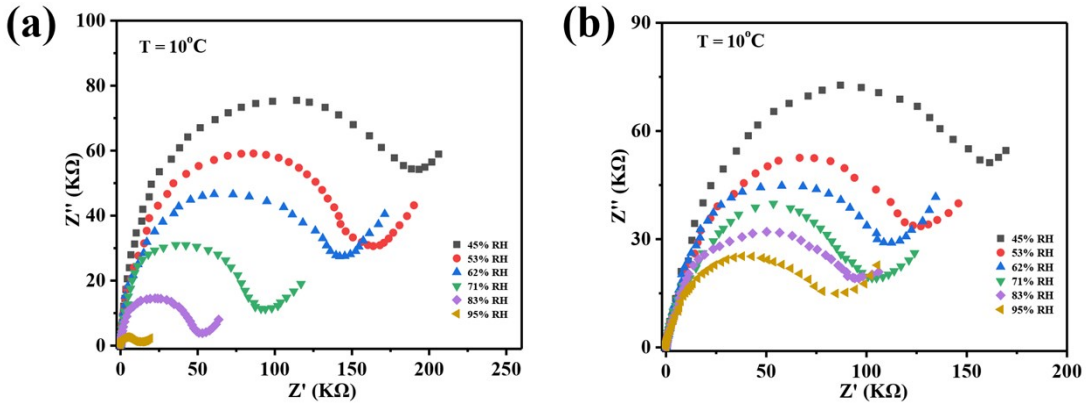

Fig. S22 (a) The Nyquist plots for polymer **1** at 10°C at different relative humidity; (b) the Nyquist plots for polymer **2** at 10°C at different relative humidity.

Detection limit calculation process:

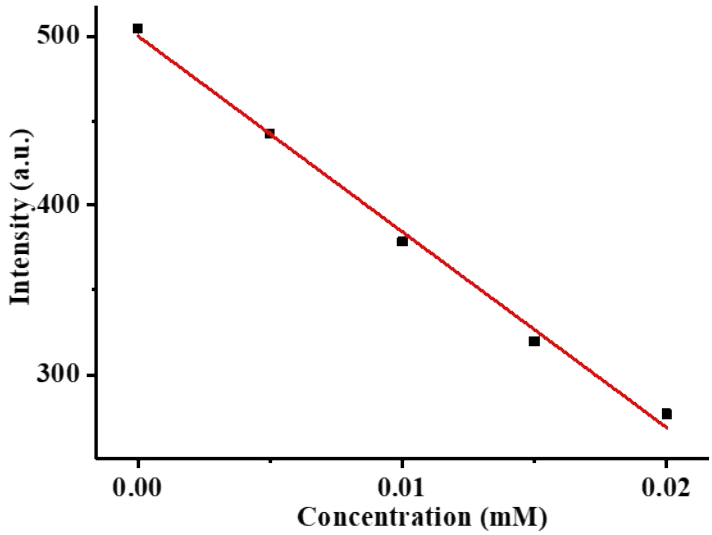

(a) Corresponding Stern-Volmer plot for polymer **1** when Fe^{3+} ions are added

Linear Equation: Y=-11566.87X+506.7

k=1.1567×10^7 M^{-1}

$$I_a=\frac{498.3+505.1+492.9+496.2+508.7+500.1+513.1+502.7+507.9+497.2}{10}=502.22$$

$$S=\sqrt{\frac{\sum(I_0-I_a)^2}{N-1}}=6.41 \quad (N=10)$$

$$LOD=\frac{3\times S}{k}=\frac{3\times 6.41}{1.1567\times 10^7}=1.66\ \mu M$$

k is the slope of the calibration curve, I_0 is the measured luminescence intensity of polymer **1** in deionized water, I_a is the average of 10 blank samples tested. S is the standard deviation of the blank group, LOD is the detection limit.

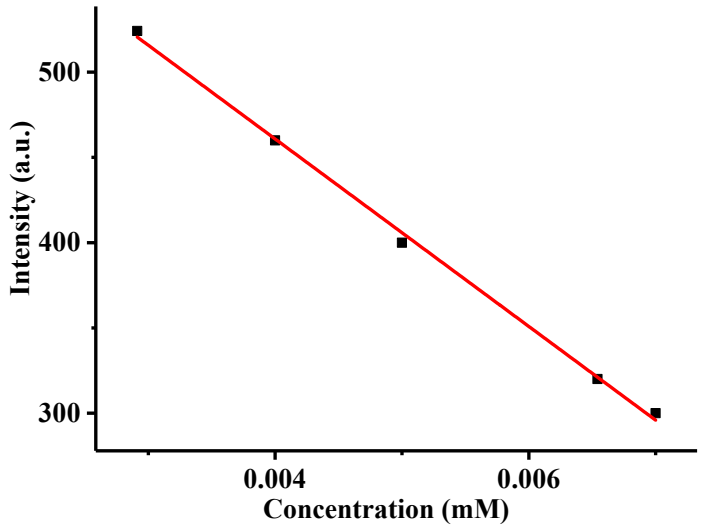

(b) Corresponding Stern-Volmer plot for polymer **2** when Hg^{2+} ions are added

Linear Equation: Y=-54978.79X+578.7

k=5.4979×10^7 M^{-1}

$$I_a=\frac{581.2+579.8+575.4+580.1+578.2+577.4+576.2+578.1+566.7+580.2}{10}=577.33$$

$$S=\sqrt{\frac{\sum(I_0-I_a)^2}{N-1}}=4.17 \quad (N=10)$$

$$LOD=\frac{3\times S}{k}=\frac{3\times 4.17}{5.4979\times 10^7}=0.23\ \mu M$$

k is the slope of the calibration curve, I_0 is the measured luminescence intensity of polymer **2** in deionized water, I_a is the average of 10 blank samples tested. S is the standard deviation of the blank group, LOD is the detection limit.

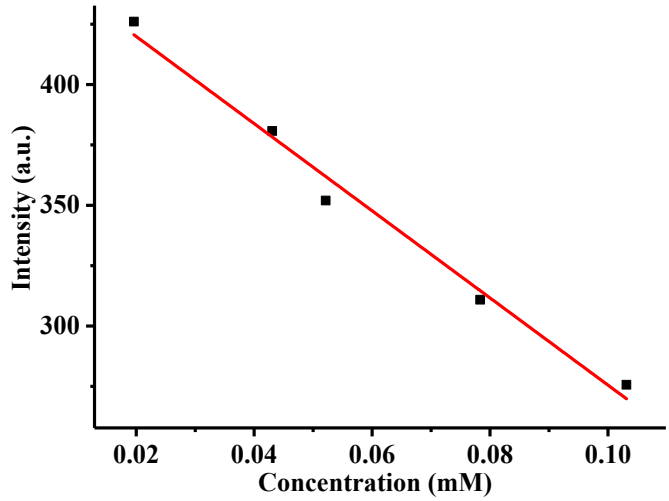

(c) Corresponding Stern-Volmer plot for polymer **1** when Fe^{3+} ions are added in biological systems

Linear Equation: Y=-1804.69X+495.2

k=1.80469×10^6 M^{-1}

$$I_a=\frac{499.7+490.2+500.1+495.4+492.3+497.4+494.5+498.1+499.4+489.7}{10}=495.68$$

$$S=\sqrt{\frac{\sum(I_0-I_a)^2}{N-1}}=3.90 \quad (N=10)$$

$$LOD=\frac{3\times S}{k}=\frac{3\times 3.90}{1.80469\times 10^6}=6.48\ \mu M$$

k is the slope of the calibration curve, I_0 is the measured luminescence intensity of polymer **1** in HEPES, I_a is the average of 10 blank samples tested. S is the standard deviation of the blank group,

LOD is the detection limit.

References

1 Y. X. Yang, S. Y. Xia, H. X. Zhang, H. H. Niu, W. J. Dong and X. X. Wu, *J. Solid State Chem.*, 2020, **284**, 121180.

2 C. G. Xu, C. F. Bi, Z. Zhu, R. Luo, X. Zhang, D. M. Zhang, C. B. Fan, L. S. Cui and Y. H. Fan, *CrystEngComm*, 2019, **21**, 2333-2344.

3 X.-Q. Wang, D.-D. Feng, J. Tang, Y.-D. Zhao, J. Li, J. Yang, C. K. Kim and F. Su, *Dalton Trans.*, 2019, **48**, 16776-16785.

4 X. M. Hou, C.-C. Yan, X. L. Xu, A.-Q. Liang, Z.-W. Song and S.-F. Tang, *Dalton Trans.*, 2020. **49**. 3809-3815.

5 Y. D. Wu, D. Y. Liu, M. H. Lin and J. Qian, *Rsc Adv.*, 2020, **10**, 6022-6029.

6 M. Chen, W.-M. Xu, J.-Y. Tian, H. Cui, J.-X. Zhang, C.-S. Liu and M. Du, *J. Mater. Chem. C*, 2017, **5**, 2015-2021.

7 T.-Y. Xu, H.-J. Nie, J.-M. Li and Z.-F. Shi, *J. Solid State Chem.*, 2020, 121342.

8 Y. Zhou, H. -H. Chen and B. Yan, *J. Mater. Chem. A*, 2014, **2**, 13691-13697.

9 M. Wang, J. G. Wang, W. J. Xue and A. X. Wu, *Dyes Pigments*, 2013, **97**, 475-480.

10 B. Wang, Q. Yang, C. Guo, Y. X. Sun, L.-H. Xie and J.-R. Li, *Acs Appl. Mater. Inter.*, 2017, **9**, 10286-10295.

11 X.-H. Zhou, L. Li, H.-H. Li, A. Li, T. Yang and W. Huang, *Dalton Trans.*, 2013, **42**, 12403-12409.

12 H. Zhu, C. Han, Y.-H. Li and G.-H. Cui, *J. Solid State Chem.*, 2020, **282**, 121132.

13 L. L. Wen, X. F. Zheng, K. L. Lv, C. G. Wang and X. Y. Xu, *Inorg. Chem.*, 2015, **54**, 7133-7135.

14 Z.-J. Wang, F.-Y. Ge, G.-H. Sun and H.-G. Zheng, *Dalton Trans.*, 2018, **47**, 8257-8263.

15 Z. Wang, J. Yang, Y. S. Li, Q. X. Zhuang and J. L. Gu, *Dalton Trans.*, 2018, **47**, 5570-5574.

16 W.-C. Kang, C. Han, D. Liu and G.-H. Cui, *Inorg. Chem. Commun.*, 2019, **106**, 81-85.

17 T. F. Xia, T. Song, G. G. Zhang, Y. J. Cui, Y. Yang, Z. Y. Wang and G. D. Qian, *Chem–Eur. J.*, 2016, **22**, 18429-18434.

18 A. Shigematsu, T. Yamada and H. Kitagawa, *J. Am. Chem. Soc.*, 2011, **133**, 2034-2036.

19 S. Parshamoni, H. S. Jena, S. Sanda and S. Konar, *Inorg. Chem. Front.*, 2014, **1**, 611-620.

20 S. Biswas, J. Chakraborty, V. Singh Parmar, S. P. Bera, N. Ganguli and S. Konar, *Inorg. Chem.*, 2017, **56**, 4956-4965.

21 X.-Y. Dong, R. Wang, J.-Z. Wang, S.-Q. Zang and T. C. Mak, *J. Mater. Chem. A*, 2015, **3**, 641-647.

22 S. Kim, K. W. Dawson, B. S. Gelfand, J. M. Taylor and G. K. Shimizu, *J. Am. Chem. Soc.*, 2013, **135**, 963-966.

23 J. M. Taylor, R. K. Mah, I. L. Moudrakovski, C. I. Ratcliffe, R. Vaidhyanathan and G. K. Shimizu, *J. Am. Chem. Soc.* 2010, **132**, 14055-14057.

24 T. Kundu, S. C. Sahoo and R. Banerjee, *Chem. Commun.*, 2012, **48**, 4998-5000.

25 R. Ishikawa, S. Ueno, S. Yagishita, H. Kumagai, B. K. Breedlove and S. Kawata, *Dalton Trans.*, 2016, **45**, 15399-15405.

26 J. N. Lu, S. F. Zhou, S. J. Zhang, C. X. Zhang and Q. L. Wang, *Eur. J. Inorg. Chem.*, 2019, **2019**, 794-799.